Chapter 2

Crystal Growth and the Reduction of Symmetry in Urea Inclusion Compounds

From Chapter 1 it is clear that the centerpiece of this research involves the study of specific properties exhibited in crystalline materials. As with any solid material, the properties of ferroelastics and ferroelectrics depend on the manner in which they were constructed or grown. Thus, some emphasis should be placed on the specific mechanisms by which these crystals grow. The purpose of this chapter is to describe studies concerned with this aspect of crystal chemistry. It begins with a short review of our present understanding of crystal growth and how specific mechanisms can induce disorder within a crystal and eventually influence its physical properties. Some forms of disorder can be controlled, and by the judicious use of tailor-made impurities, macroscopic crystal properties such as the development of specific crystalline faces and the reduction of crystal symmetry can be influenced. Thus, the construction of *mixed guest* UICs by the addition of a second guest impurity that is structurally similar to the first has received much attention. Studies on the incorporation guest impurities have broadened our understanding of UIC growth and guest ordering.

2.1 The Terrace-Ledge-Kink Model of Crystal Growth

The majority of crystals are grown under conditions that do not favor thermodynamic equilibrium. The continuous reduction in solution temperature (by cooling) or volume (by evaporation) provides insufficient time for equilibrium to be achieved, so the process is predominantly a kinetic one.[1,2] When a crystal grows, it does so by adding new material (molecules or atoms) to its surfaces. As growth continues

these surfaces become covered so that what was once the surface of a crystal soon becomes buried under new growth. Once this happens, the potential for reorientation or dissolution is reduced and defects or disordered sites can become permanently incorporated into the crystal.

The growth of many crystals is thought[3,4] to occur according to the "terrace-ledge-kink" (TLK) mechanism, depicted in Figure 2.1. As a crystal is growing in size from a small number of molecules to a macroscopic entity, it does so in a fashion that minimizes the number of high-energy sites on it surfaces. For growth units that are considered isotropic, the energetic potential of a growth structure on the surface of a crystal is proportional to its solvent-exposed surface area. Generally, surface features with greater surface area in contact with the crystal will expose less area to the solvent. Therefore, stable crystal growth occurs at sites on the crystal where newly grown structures can maximize their contact with the crystal surface. On the molecular scale, a crystal surface consists of many kinds of interfaces between crystal and crystallizing solution. As Figure 2.1 illustrates, some sites of attachment provide weak associative contact with the rest of the crystal. "Terrace" and "ledge" sites interact with one or two surfaces, respectively, of a newly added atom or molecule. However, because they share three surfaces, atoms or molecules that attach to the "kink" site of a growing crystal exhibit greater interaction with the growing crystal. Atoms or molecules that attach to kink sites are more resistant to dissolution than those at either terrace or ledge sites; permanent crystal growth therefore occurs preferentially at these locations. The TLK model asserts that crystal growth at the kink site will reduce the exposed surface area at that region. Of course, the

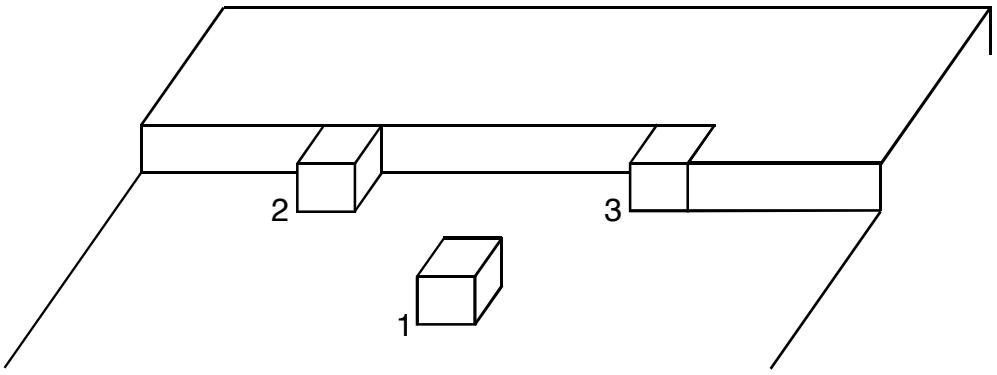

Figure 2.1 A cartoon depicting the terrace-ledge-kink (TLK) mechanism of crystal growth. A building block located on the terrace (1) makes minimal contact with the crystal surface; growth at this position is metastable, and dissolution of the block by surrounding solvent is likely. Instead, the block may attach at a ledge on the crystal (2) where it adjoins the crystal with two surfaces and gains greater stability. The most favorable growth occurs at the kink site (3), where the building block makes contact with the crystal at three surfaces. Growth at the kink site should exhibit the greatest stability and the least likelihood of dissolution. Figure drawn from Wadhawan, V. K. *Introduction to Ferroic Materials*, (Taylor and Francis, New York, 2000), p. 35.

process of “filling in” one kink site usually results in the formation of another so that this process may be regarded as being self-propagating.

2.2 Circumferential Crystal Growth and Inclusion Characteristics

Although not composed of isotropic building blocks, urea inclusion compounds are thought to grow according to the TLK theory. However, the precise mechanism for UIC growth depends on crystal symmetry and local structure at the growth interface, both of which ultimately dictate patterns of guest incorporation. Since guest zoning can affect properties such as ferroelasticity and optical behavior, in order to fully understand the physical properties of UICs, one must appreciate their growth mechanisms. Such studies are described below.

2.2.1 The Incorporation of Crystal Impurities Can Reduce Crystal Symmetry

Crystals grown in single-component solutions, though common in many chemistry laboratories, are but a subset of attempts at crystallization. Indeed, for the synthetic or industrial chemist, crystallization is a means by which one component can be removed and purified from a solution of several. Although it has long been accepted[5] that impurities can affect the growth of crystals, only recently has an understanding of this process become available.

When a crystal is growing, it usually does so under non-equilibrium conditions.[2] Slow cooling or evaporation of saturated solutions are two common methods by which crystals are grown. Both of these methods force the system to supersaturation so that

reversibility in crystal growth is disfavored. Thus, once an atom or molecule becomes attached to the growing crystal, removal or rearrangement may be difficult.

In a crystallization solution composed primarily of one component plus small amounts of an additive, crystal growth of the primary component, or *host*, will tend to occur so that the preferred symmetry of this crystal is exhibited. This means that each atom or molecule of host will be related to others by symmetry rules applicable to the pure crystal. (Exceptions to this behavior can arise from the effects of incorporated impurity on the attachment of host molecules.[6]) Should the additive itself be incorporated into the host crystal, it too will be located at sites governed by the symmetry of the host. However, the additive, or *guest*, does not necessarily have the same molecular (or atomic) shape or crystal growth characteristics as the host. Because it is incorporated at the surface of the growing crystal, the presence of guest may perturb the local symmetry of the crystal and alter the growth characteristics so that the overall symmetry of the resulting *solid solution* is not the same as for the pure material.[1]

This process is summarized in the elegant cartoon of McBride[7] (Figure 2.2). In this figure, a crystal lattice of host "ducks" is depicted as growing in the presence of guest "ducks." Although similar to the hosts in shape and size, these guests differ slightly from the host due to a protrusion from the backs of their heads. In this crystal, ducks pack so that their heads interdigitate; this protrusion can reasonably be expected to alter the molecular recognition for the guests. Between two hosts, interlocking of their complementary heads appears facile. However, the protrusion from a guest's head gives rise to a repulsive interaction between host and guest.

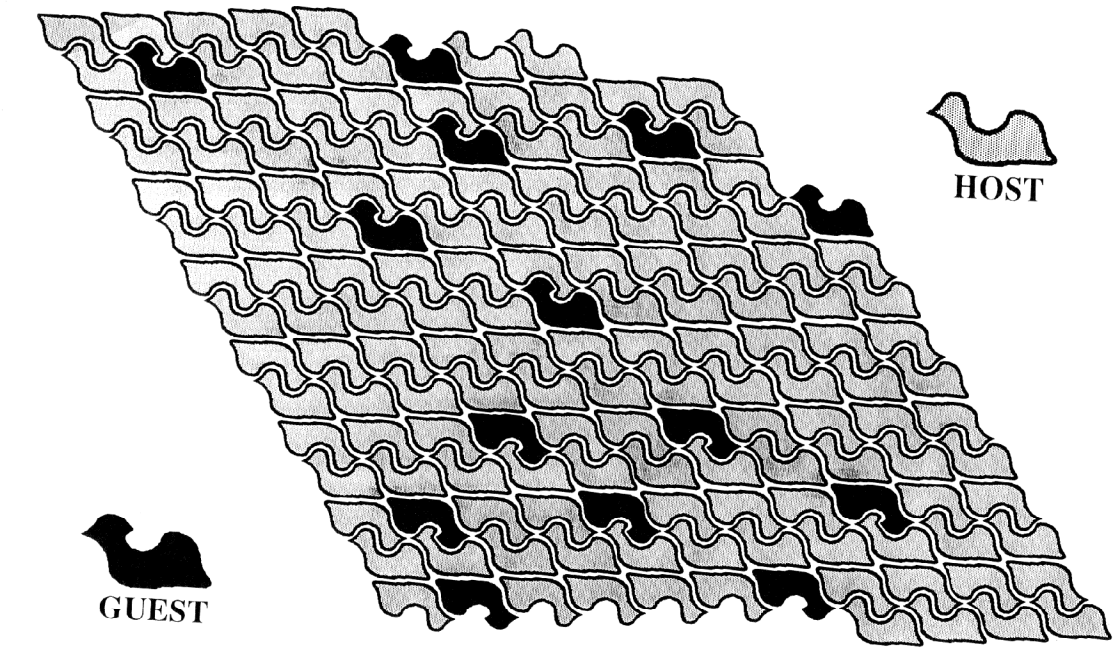

Figure 2.2 Symmetry reduction in solid solutions. The differences in molecular recognition exhibited by host and structurally similar guest lead to preferential incorporation at growth faces that depends on the symmetry of those faces. Here, those differences suppress incorporation of guest at the right and left faces but allow incorporation at the top and bottom face. Such preferential incorporation leads to a reduction in crystal symmetry: here, unidirectional ordering of guest within the top and bottom sectors makes them polar. See text for a more thorough discussion. Figure taken from McBride, J. M. *Advanced Materials*, (1989), *1*, 87-89. Copyright Wiley-VCH Verlag GmbH & Co. KGaA. Reproduced with permission.

This minor change in molecular shape can appreciably influence the molecular recognition process. For instance, along the right face of this crystal, growth occurs at the kink site near the top. For growth to proceed at this site, the next duck to attach must attach "head first" onto the guest duck that occupies the site. This event is disfavored thermodynamically, but the kinetic control of crystal growth under supersaturation dictates that growth must persist. This might involve attachment and associated deformation of a host duck or dissolution of the offending guest and replacement by a host. Because it involves no structural perturbation of subsequent ducks, the latter option is anticipated for this site. In this case, some reversibility in crystal growth is tolerated because the guest duck was only temporarily associated with the surface. This reversibility allows the right and left quadrants of this crystal to become composed almost entirely of hosts so they resemble in structure the "pure" crystal.

The top and bottom faces of the crystal present an entirely different situation. On the top surface, guest ducks such as the one shown can attach through their bottom sides without immediately deforming the crystal or interrupting crystal growth. Further growth (along the horizontal direction) will continue so that structural perturbation by the guest impurity becomes apparent only as the next row of ducks is constructed. By this time, the guest duck is well entrenched: it is locked into position by the host to its immediate right. Removal of this impurity would require dissolution of adjacent host or hosts and is therefore unlikely. Although energetically costly, host ducks can accommodate the guest protrusion so that overgrowth of this site may occur, but growth along this face should be slowed. In the end, however, guest impurities can become permanently incorporated into this crystal face.

This schematic illustrates the preferential incorporation of guest impurities into different growth faces. The symmetry at the crystal growth surface does not possess all of the elements of the bulk, so guest molecules will associate differently with faces that do not share the same symmetry. In this schematic crystal, a twofold rotation axis extending through the page relates the top face to the bottom and the right face to the left. These sets of symmetry-related faces exhibit similar characteristics of guest incorporation that differ between the two pairs. Growth at the left and right faces is much less affected by the guest, whereas guest incorporation along the top and bottom faces both slows growth and results in a lowered internal symmetry. Slower growth at these faces may be reflected in the crystal habit: the crystal may appear wider (in relation to its height) than it would be if grown in the absence of guest.

The important point here is that incorporation of guest impurities can reduce the symmetry of the crystal in which they are included. In Figure 2.2, the point symmetry of the two-dimensional lattice of host ducks is 2. Because guest incorporation occurs preferentially at certain faces, the crystal can now be dissected into four sectors along the diagonals. (The intersection of these diagonals occurs at the crystal nucleus.) Such a dissection defines two kinds of sectors for this crystal. The left and right sectors, in which there are no incorporated guests, retain the twofold symmetry of the pure host crystal. However, for the top and bottom sectors, the inclusion of guest impurity occurs in a directional fashion. The result is the growth of sectors with point symmetry of 1. In addition, the nonrandom orientation of the guest ducks in the top and bottom growth sectors makes these sectors polar.

The work of Addadi, Lahav, Leiserowitz, and coworkers shows that the addition of 'tailor-made' auxiliaries can result in the selective inclusion of cinnamic acid[8] and thienylacrylamide[9] into cinnamide hosts, the preference of one amino acid enantiomer over another in the prochiral faces of glycine,[10,11] and enantiomeric resolution by selective inclusion.[12] Other workers have contributed to this exciting field. McBride and Bertman[13] demonstrated that the symmetry reduction exhibited in solid solutions of hosts that naturally grow as high symmetry (optically uniaxial) crystals could be easily studied under the polarizing microscope. Their observations led to the brilliant work of Kahr and McBride,[1] who summarized 150 years of optical crystallography in their treatise on "optically anomalous crystals." These workers demonstrated that symmetry reduction in the solid state is not necessarily detectable by routine X-ray crystallography. In such systems, they caution, "X-ray diffraction can mislead by providing a crystal structure that is averaged over several domains." The polarized light microscope, they continue, can provide fast, accurate information on crystal symmetry and domain structure, and can help to "identify regions in a solid that are worth more detailed study by other techniques."

This work set the stage for more comprehensive studies into molecular recognition of mixed crystals. Initially, guest impurities were chosen for their similarity to the host. However, Kahr and coworkers have demonstrated that such a constraint is unnecessary. These investigators and others have shown that mixed crystals may be grown of simple salts and drastically different constituents,[14] including organic dyes[15-17] and proteins.[15] For example, crystals of potassium sulfate and barium acetate were shown to include a variety of fluorescent sulfonate- and carboxylate-substituted aromatics.[18]

These studies were undertaken to probe the molecular properties of the aromatic guest when confined to the host lattice and have been extended to studies on the adsorption of chiral biphenyl derivatives in anisotropic media.[19]

2.2.2 Zoning of Guests in Urea Inclusion Compounds

The crystal symmetry of urea inclusion compounds is, as for other crystals, subject to the restrictions that nature places upon it. As shown by the work of Lahav and others (Section 2.2.1), anisotropy at the face of a growing crystal can lead to differences in molecular recognition for various types of molecules. As will be demonstrated, structural differences at the growth faces can lead to interesting incorporation features of structurally related guests.

The growth mechanism of a crystal involves the incorporation of material in a manner that is related to the microscopic symmetry of the crystal *at the growth face.* When the symmetry at the growth face is not the same as the overall crystal symmetry, differences in molecular recognition become evident. For many urea inclusion compounds, the host channels have nominal sixfold rotational symmetry in the plane perpendicular the channel axis. However, when viewed along its longest axis, an aliphatic guest has mirror plane symmetry along its polymethylene chain. For a UIC in which the guests are completely disordered, there exist many options for the alignment of the guest chains.[20-22] However, for UICs containing diketones or certain monoketones, hydrogen bonding between host and guest can lead to alignment of at least a portion of the guest chain toward the channel wall. Ordering of guests toward channel walls limits the number of directions along which the polymethylene chains may be pointed. In 2,10-

undecanedione/urea (space group $C222_1$), guest chains are oriented toward {100} channel faces. Within a channel, guests are related by the twofold screw axis so that there are only two directions along which guest chains are oriented. Alternatively, in 2,9-decanedione/urea (space group $P3_112$ or $P3_212$), guests are related by the threefold screw axis that runs parallel to the channel. Here, there are three directions along which guests are oriented.

In Section 2.2.1, it was established that when the symmetry of the growth face is different from that of the crystal, differences in molecular recognition at various growth faces may occur. Variations in inclusion, referred to as *zoning*, provide the experimentalist a handle with which the crystal growth process may be investigated and possibly controlled. In general, there are two varieties of guest zoning relevant to this discussion.[18] When zoning occurs between growth sectors whose faces are not related by symmetry, the work of Lahav, McBride, and others has shown that different guests may be unevenly partitioned between these sectors. This phenomenon is known as *intersectoral zoning*. With intersectoral zoning, differences in guest incorporation are observed between distinct growth faces of the same crystal. However, within symmetry related growth faces, there may exist differences in the exposed surface topography.[14] When variations in guest content occur *within* the same growth sector, the phenomenon is known as *intrasectoral zoning*. Both kinds of zoning have been observed in a variety of solid solutions and mixed crystals. Urea inclusion compounds containing two guests of similar molecular size and shape can also be considered solid solutions. Because they are subject to the same phenomena of crystal growth and impurity distribution as other solid

solutions, one might expect many examples of guest zoning in UICs. Some of these will be discussed below.

2.2.3 Crystals of Trigonal Symmetry

2.2.3.1 Trigonal Growth and Guest Zoning

Urea inclusion compounds of 2,9-decanedione exhibit trigonal crystallographic symmetry, with $3c_g' = 4c_h'$ and space group $P3_112$ or $P3_212$, depending on the handedness of the channel. (Refer to Section 1.1.2 for a more thorough discussion of 2,9-decanedione/urea.) Similarly, 2,12-tridecanedione/urea has $3c_g' = 5c_h'$ and space group $P3_112$ or $P3_212$. For both crystals, the commensurate host-guest repeat spans three guests that are related to one another by a threefold screw axis along the length of the channel. As described below, the type of guest and its many possibly interactions with the urea channel play a decisive role in the structure and properties of the UIC.

When a guest molecule attaches to the growing channel, it will interact with the exterior surface through a variety of intermolecular forces. Certainly one of the strongest and most directional of the attractive forces available to non-ionic molecules is the hydrogen bond,[23] which can form between the guest carbonyl and a urea donor. Suitable hydrogen bond donors are found on the growth face; they are provided by ureas that have rotated about their C=O axes so that they may form hydrogen bonds with guests in the outermost completed channels. Before the new channel is formed, these ureas can presumably expose their second NH_2 groups to surrounding solvent (typically, methanol with trace amounts of water). As the new channel grows, the formation of a host-guest hydrogen bond can strongly affect the longitudinal positioning of the initial guest

"template" on the exterior surface of the crystal. Thus, new guests should be arranged so that hydrogen bonding can occur with an appropriate urea on the outer channel wall. This arrangement also appears favorable for the urea since the energetic cost of breaking hydrogen bonds with other ureas is offset by rotation about the twofold axis to form hydrogen bonds with guest and solvent.

A possible mechanism for growth of commensurate UICs with trigonal symmetry is provided in Figure 2.3.[24] For these crystals, three guest "layers" comprise a single commensurate repeat; in this depiction, layer 1 lies below layer 2, which lies below layer 3, etc. (Because of the trigonal symmetry, layer 4 is oriented the same as layer 1, etc.) Although channels of either helical sense are possible, the crystal structure of 2,9-decanedione/urea shown in Section 1.1.2 was solved as a right-handed urea helix (Figure 1.5). Along this channel the guest coils in a counterclockwise fashion with an internal carbonyl torsion angle (O=C---C=O) of 106°.[25] Thus, ketones on opposite ends of the same guest form hydrogen bonds with ureas on adjacent channel walls, as depicted in the helical wheel diagram shown in Figure 1.8f.

In the proposed model, hydrogen bond formation between guest and ureas on neighboring channel walls determines the orientation of incorporated guests. Because hydrogen bond donor ureas are exposed at the kink site, it is the donor ureas (specifically, those in the layer below the kink site, or *underlayer*) that dictate the molecular recognition of the kink site. In Figure 2.3a, donor ureas (solid wedges) immediately under layer 1 are directed toward the upper right channel wall. In the crystal structure of 2,9-decanedione/urea, ureas form hydrogen bonds with guests on both sides of the channel wall (Section 1.1.2), so these ureas are already associated with guests in adjacent

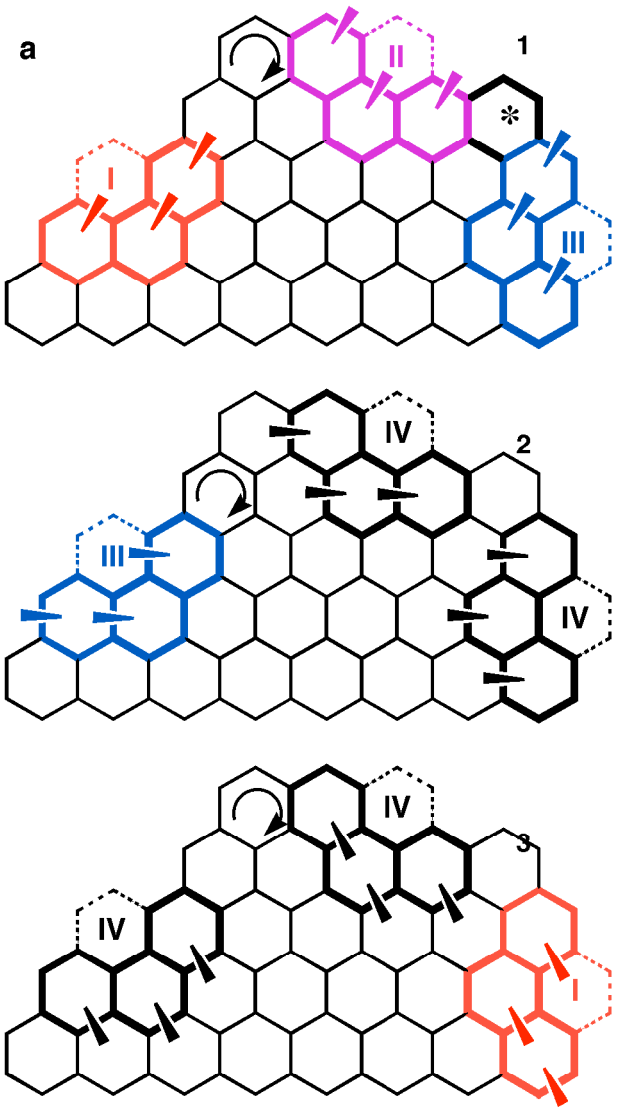

Figure 2.3 The proposed mechanism for growth of UICs containing 2,9-decanedione and an impurity. (This mechanism should also be applicable to other UICs exhibiting trigonal symmetry.) **(a)** A cartoon of the three underlayers in the host substructure of each commensurate repeat. In this depiction, layer (*n*+1) lies in front layer *n* so that layer 3 is closest to the viewer and layer 1 is below layers 2 and 3. For each, a urea in the *underlayer* is available to donate hydrogen bonds to incoming guests; these are depicted with a solid wedge (◄). Hydrogen bond formation between ureas in the underlayer and guests in a growing channel is thought to dictate molecular recognition at the growth kink site, and hydrogen bonding ureas can be exposed to the kink site in one of four ways (I, II, III and IV). In this diagram, kink sites are drawn with dotted lines. Over each commensurate repeat, the kink sites along the left and right faces expose the same host molecular functionality (sites I, III and IV), while the top face exposes sites II, IV and IV. On this basis, the top face is thought to incorporate (zone) and/or order guests differently. **(b)** A cartoon illustrating the pattern of intersectoral zoning predicted for the crystal in **a**. Differential guest incorporation is anticipated to occur between growth faces of different color, while faces of the same color are expected to include guests in a similar fashion. This crystal is composed entirely of dextrorotatory (d) helices (an arbitrary assignment). However, some crystals include levorotatory (l) channels, as well. For this mechanism, a change in handedness is predicted to reverse the pattern of guest recognition so that at a chiral twin boundary type A faces become type B faces, *etc.* One possible scenario is depicted in **c**. Here, the right sector is composed of channels of both handedness so that the sense of guest inclusion is reversed at the chiral twin boundary (violet line).

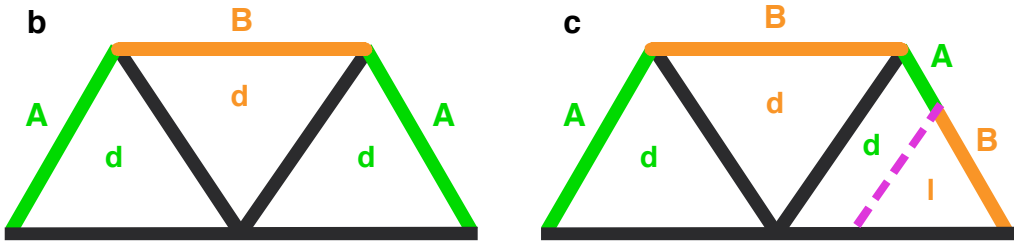

channels and will expose NH groups into the kink site. As guests become incorporated into the growing channel, hydrogen bonding with these ureas dictates the orientation of guests (and the location of donor ureas) at the kink site.

As growth continues, hydrogen bonding between host and guest can govern the molecular recognition exposed at the kink sites. For the crystal in Figure 2.3, the addition of new channels occurs in the sense of a right-handed growth spiral. (A change in either the sense of growth spiral or the handedness of the channels does not alter the argument presented here, but does change the sense of guest rotation. This is addressed below.) During growth, each face of this crystal is presumed to have at least one kink site at which new channels are constructed (dotted lines). Each kink site is bounded by three complete channels, each of which may include a urea that has rotated about its C=O axis to form hydrogen bonds with the incoming guest. Since hydrogen bonding with two guests is preferable to one, ureas positioned for donating to guests in the completed channel are more likely to donate hydrogen bonds to a guest in the growing channel; this results in a difference in exposed molecular functionality at the respective kink sites that depends on the longitudinal position of potential donor ureas. By following the progression of donor ureas over the three layers in the unit cell, it should be possible to identify these differences. When a donor urea lies along the leading edge of the growth spiral, it is denoted a type I urea (shown in red). The molecular recognition for type I ureas should differ from type II (violet) and type III (blue) ureas, in which the donor that occupies the kink site is oriented 60° or 120° away from the growth direction. Sometimes, a growing layer will expose no donor ureas at the kink site; these are known as type IV sites (shown in black). Over the course of a complete commensurate repeat

(unit cell), the sum of donor urea sites should dictate the overall properties of molecular recognition at kink sites on a particular growth face. Such changes in molecular recognition may include preferential incorporation of guests that results in intersectoral variation of guest stoichiometry and/or differences in ordering of one guest over the other (for instance, an orientational preference for one of the guests). In the figure, the left and right faces exhibit one each of type I, III and IV sites. When summed over the unit cell, growth along these faces appears to expose the same molecular functionality and should therefore exhibit similar properties of molecular recognition and guest incorporation (partitioning) or ordering. However, the top face exhibits type II and IV sites; thus, the molecular recognition should differ for this face. For this discussion, the left and right faces are arbitrarily denoted type A faces, while the top face is arbitrarily denoted a type B face.

For a UIC grown from a solution containing a mixture of 2,9-decanedione and 2-decanone, type A and type B faces should recognize these guests differently. This mechanism does not predict the fashion in which preferential incorporation or ordering will occur; it only predicts a difference. (One might presume[26] that type IV sites are less able to attract hydrogen bond acceptors than are types I, II or III; however, this hypothesis has not been tested.) Nevertheless, such a mechanism has been instrumental in rationalizing patterns of guest zoning in mixed UICs containing 2,9-decanedione.

Crystal twinning should have an effect on molecular incorporation, as well. In UICs, both rotational and chiral twinning are possible. For a crystal consisting of a single unit cell orientation and sense of helicity, the mechanism proposed above predicts different patterns of guest recognition for adjacent faces and similar patterns for

alternating faces, as illustrated in Figure 2.3b. These differences arise because the unit cell is oriented differently with respect to the growth face, but rotational twinning can alter the simplistic predictions described in Figure 2.3.

Between rotational twins, the change in unit cell orientation should give rise to changes in molecular recognition exposed at the kink site. For example, variations in unit cell orientation within a growth sector should lead to differential guest incorporation or ordering. In another scenario, rotational twinning can allow different faces to expose the same molecular functionality. One way to appreciate this is to consider the angle between the unit cell and the growth face. When this angle is preserved between faces (due to rotational twinning), these faces should incorporate (or order) guests in the same fashion. When this angle is not preserved (for instance, between twins grown on the same face), molecular recognition (and, therefore, guest incorporation and/or ordering) should differ. However, the trigonal symmetry of 2,9-decanedione/urea should render 120° rotational twins equivalent when they are on the same growth face; twins that are not related by 120° should exhibit differential guest incorporation and/or ordering. (This point is addressed in Section 2.2.3.2.)

Because chiral twinning produces a diastereomeric kink site, it also should affect the sense of molecular recognition. In a UIC, urea channels are packed together in the plane perpendicular to the channel axis. Differences in optical rotation due to chiral twins are observable in this plane; for UICs containing 2,9-decanedione or 2,12-tridecanedione, such twinning can be observed when viewing through an {001} face in the polarizing microscope. As of yet, the sense of channel helicity and optical rotation have not been correlated unambiguously, so it is unknown whether right-handed channels

are dextrorotatory or levorotatory. (Although Schlenk[27] predicted a correlation between optical rotation and the sense of the urea helix, no unambiguous data have been presented on this matter.) The mechanism outlined in Figure 2.3a assumes crystals of uniform chirality. Because right-handed and left-handed channels are enantiomorphous, one might anticipate that changing the handedness of the helical channel while keeping the sense of circumferential growth constant would change the spatial relationship of the donor ureas and acceptor guest ketones to the kink site. This is exactly the case predicted by this model: the presence of a chiral twin "reverses," in effect, the characteristics of molecular recognition at the growth face. Figure 2.3a depicts right-handed channels; for left-handed channels the sense of winding for the guest along the channel will be reversed so that the orientation of ketones in each layer is changed. Should this occur, the molecular recognition at type A faces will become those of type B, and type B faces will act as though they were type A. In short, the pattern of guest incorporation will become reversed. One conceivable example is depicted in Figure 2.3c; here, the rightmost face of the crystal consists of two enantiomorphous halves (one dextrorotatory and the other levorotatory). (In this example the chiral twin boundary is drawn so that it intersects the growth face at an angle of 60°. To date, the chiral twin boundaries observed in trigonal UICs have all been oriented along {110} faces, which may be found at this angle or parallel to the growth face.) The model for trigonal growth predicts the pattern of recognition will be reversed at the chiral twin boundary so that if one twin within the sector is type A, the other will be type B. Thus, it may be possible to identify chiral twinning on the basis of the guest zoning it induces.

To this point, the discussion of growth has assumed growth along growth spirals[4] (or some other directional construct) and that the helical sense of these spirals is conserved throughout the crystal. (Although such spirals have not been observed directly,[26] this model assumes their presence.) It is also possible that the sense of the growth changes during crystal growth. Should this occur, the location of the kink site will change, and this should affect the molecular recognition of guests. For instance, in Figure 2.3a, the crystal is drawn with a right-handed sense of growth (new channels are added in a fashion that follows a clockwise circular motion). Considering only the rightmost face, the molecular functionality exposed at the kink site (dotted lines) of this face is III, IV and I for layers 1, 2 and 3, respectively. If, for this sector, the sense of the growth spiral is reversed from right- to left-handed, the location of the kink site for the rightmost growth face will move to the top side of the face (see channel with asterisk in layer 1). At this kink site, the upper donor urea is oriented 60° to the direction of growth in layer 1, while layers 2 and 3 do not expose donor ureas to the growth site. Thus, the molecular functionality becomes II, IV and IV for layers 1, 2 and 3, respectively, and the face is now type B. Similar changes can be predicted for the other faces so that guest recognition for this crystal becomes reversed for each. Thus, a change in growth sense at the boundary between the top and right faces in a crystal that would otherwise incorporate (or order) guests according the pattern A-B-A would result in the pattern A-B-B.

2.2.3.2 Optical Evidence of Guest Zoning

Optical studies on mixed crystals are a rich source of information on guest zoning, and ordering characteristics and have provided evidence in support of the growth mechanism proposed in the previous section. The utility of the optical microscope in the study of crystals and solids has been well documented.[1,28,29] Most commonly, crystals are studied using the polarizing microscope, which involves mounting between a pair of polarizers oriented at 90° (*crossed*) with respect to each other. This arrangement allows one to observe many important details about the symmetry of a crystalline specimen. A brief discussion of crystal optics follows.

When plane-polarized light passes through a crystal, the light is separated into two components (eigenrays). For a crystal that is oriented at an extinction angle of 45°, the intensity, I, of transmitted light is described[30,31] by the equation,

$$I = I_0 \cdot \sin^2\left(\frac{\delta}{2}\right), \qquad (1)$$

where I_0 is the intensity of the incident radiation and δ is the phase shift between the eigenrays at a given wavelength, λ. When passing through a birefringent crystal, these waves become out of phase, and their separation, or *retardance*, is defined[30,32] as,

$$\Gamma = \frac{\delta\lambda}{2\pi} = L \cdot \Delta n, \qquad (2)$$

where L is the path length and Δn is the difference in refractive index between perpendicular waves.

In particular, the Metripol birefringence imaging transmission microscope[33] has provided many fine details concerning guest inclusion not readily available from other

methods. Briefly, this instrument utilizes the rotating polarizer method[32] to measure the birefringence of crystalline samples. It is capable of estimating the linear phase shift between eigenrays (δ) as $|\sin \delta|$ and slow axis orientation (ϕ) for a sample from data collected at one of several wavelengths. By combining data collected at three wavelengths, it is possible to determine the absolute phase retardation.[32] Orientation images are colored in a fashion that corresponds to the scale of first-order interference colors normally observed in a polarizing microscope (as represented in a Michel-Levy chart[34,35]). Using phase shift data (δ) obtained from Metripol birefringence images, it is a simple matter to determine the retardation of a sample using equation (2). Since they are related by the factor $\lambda/2\pi$, the discussion of crystal optics uses concepts "retardation" (Γ) and "phase shift" (δ) almost interchangeably.

Owing to their symmetry, urea inclusion compounds of either 2,9-decanedione or 2-decanone are optically uniaxial. However, UICs containing mostly 2,9-decanedione and small amounts of 2-decanone are biaxial. For these optically anomalous crystals,[1] the observed linear birefringence is a function of the directionality and magnitude of the crystal's refractive index tensor and is thought to result from the anisotropic distribution and/or orientation of the two guests within the crystal. For a UIC containing more than one guest, differences in guest content or ordering between sectors (or twins) should be observable as differences in retardation. A particularly fine example is shown in Figure 2.4. This crystal was grown (by Mark Abel[36]) in a slowly cooled methanol solution containing urea and a 90:10 mixture of 2,9-decanedione and 2-decanone. The photomicrographs demonstrate biaxial growth sectors whose interference colors change as a function of crystal orientation. For most UICs containing mixtures of 2,9-

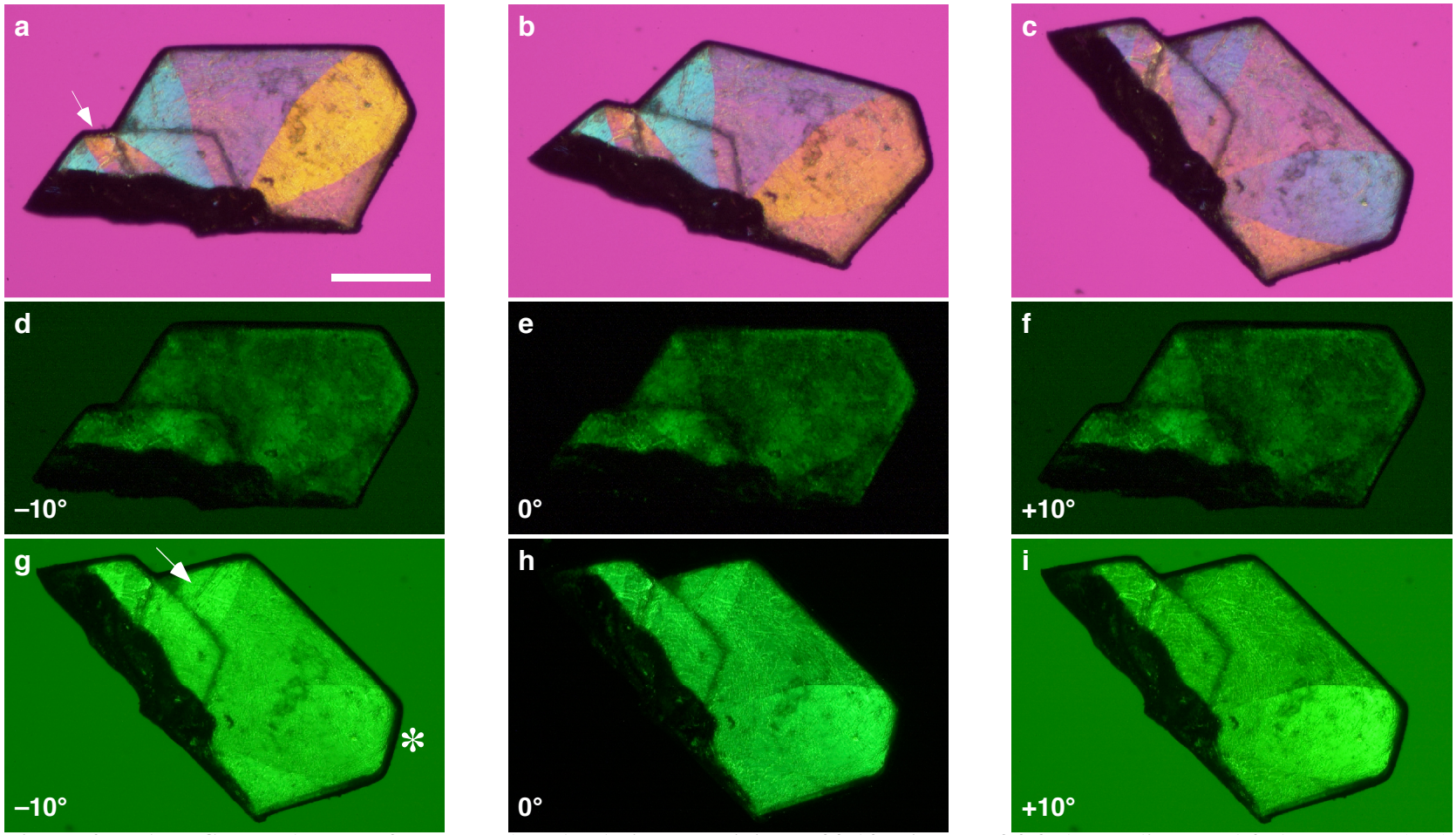

Figure 2.4 A UIC crystal grown from a methanol solution containing a 90:10 mixture of 2,9-decanedione and 2-decanone. **(a-c)** Photomicrographs of the crystal, taken between crossed polarizers and λ plate, at 0°, +15° and +45° relative crystal orientations. These photos illustrate the optically anomalous nature of the crystal. Scale bar = 500 μm (Nikon 2.5x). **(d-f)** Photomicrographs taken between nearly crossed polars and with green interference filter. The crystal is oriented as in **a**. For these photos the analyzer has been rotated to –10, 0 and +10°, respectively. In **d**, dextrorotatory regions appear darker than in **e**, while in **f**, darkened regions are levorotatory. **(g-i)** Photomicrographs analogous to **d-f**; the crystal is oriented as in **c**. In **g**, chiral twinning is observable in one sector (see arrow). The asterisk indicates a region for which the retardation appears to change within the sector. This region is explored in Figure 2.5.

decanedione and 2-decanone, the interference colors are not as intense nor is growth sectoring so well defined; for this crystal, both are clearly observed.

Since the linear birefringence is so weak, optical rotation arising from this chiral crystal can be observed. In photomicrographs shown in Figure 2.4d-f, the orientation of the analyzer has been rotated (from perpendicular to the polarizer, or *crossed*) by -10°, 0° and +10°, respectively. By noting changes in the transmission of light for each position of the analyzer, it is possible to determine the sense of optical rotation for crystal sectors or portions thereof. (The green background results from the green interference filter that was inserted into the light path. This filter eliminates problems arising from variation in optical rotation with wavelength (optical rotatory dispersion) and therefore increases the contrast between enantiomorphous regions of the crystal.[37,38]) For photomicrographs taken with the Nikon microscope, regions that appear darker as the analyzer is rotated to "negative" values (*e.g.*, -10° from crossed) are dextrorotatory (*d*).[39] Analogously, regions that appear darker at "positive" analyzer orientations are levorotatory (*l*). Although underexposed (the camera shutter speed was not fixed, as it should have been, during the collection of these images), photomicrographs d-f illustrate that the majority of the crystal is levorotatory. (Adjustment with software of levels and brightness improve the brightness of these images, but only at the expense of clarity. For the images presented, no software adjustments have been performed.) In some cases, photomicrographs must be collected for more than one orientation of the crystal to confirm rotational assignments. For instance, intensity within the top left sector does not change appreciably over the series of images in Figure 2.4d-f. With the exception of the chiral

twin that is discussed below (see arrow in Figure 2.4g), photomicrographs g-i demonstrate levorotatory behavior for this sector.

Birefringence images of this crystal are provided in Figure 2.5. At first glance, growth sectors in this crystal appear to exhibit the alternating pattern in |sin δ| discussed in Figure 2.3. Other possible sources of optical behavior should be considered against the trigonal growth model, which was introduced in terms of a consistent unit cell orientation throughout the crystal. The model asserts that differences in the angle at which the unit cell intersects the growth face will yield changes in molecular recognition at the kink site. Such changes can result from rotational twinning within a single crystal growth sector. It therefore becomes important to make the distinction between rotational twinning and growth sectoring. In growth sectoring, different interference colors exhibited in various sectors arise from differential incorporation of the major and minor guests into the various recognition sites that are presented at each of the growth surfaces. This rotation of the slow axis occurs without concomitant rotation of the unit cell axes. At the same time, however, rotational twinning can lead to differences at the kink sites because the unit cell changes orientation with respect to the growth face. As discussed in Section 2.2.3.1, rotational twins that preserve the relationship between the unit cell and the growth face should exhibit similar patterns of guest incorporation and ordering.

Since the origin of optical anisotropy in UICs containing 2,9-decanedione and a guest impurity is not understood, a simple way to test the validity of the growth model is to use it to rationalize patterns in the optical properties of this crystal (and others). Whereas with growth sectoring, the boundaries between different orientations will coincide with the sector boundaries, rotational twinning may occur over a variety of

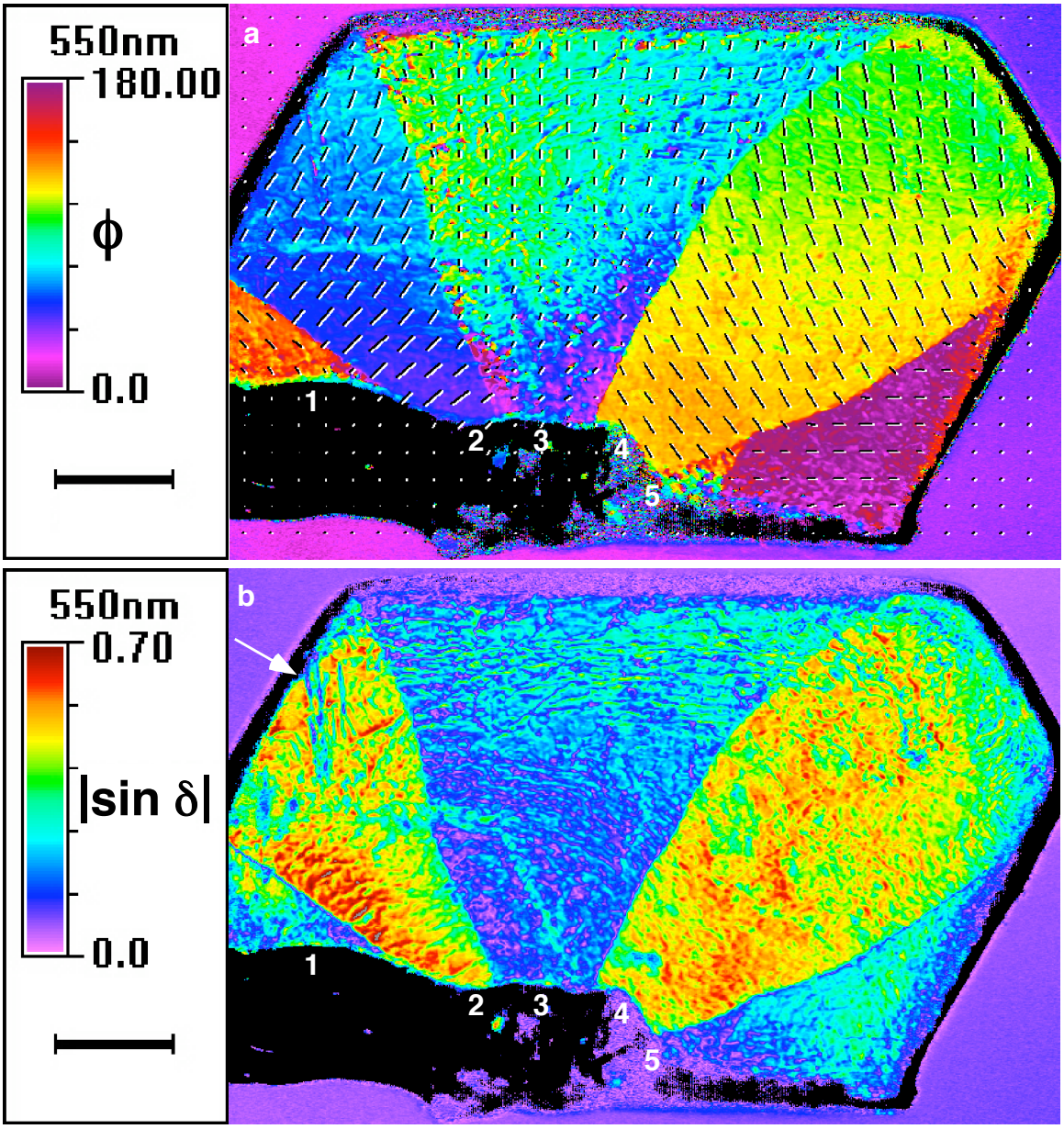

Figure 2.5 Birefringence imaging of the crystal presented in Figure 2.4, collected at 550 nm incident wavelength. **(a)** Orientation map. Approximate slow axis orientations are denoted by the arrows. Although difficult to resolve here, chiral twinning in the upper left sector (Figure 2.4g) is clearly visible in the phase retardation map, **b** (see arrow). Scale bars = 230 μm (Metripol 4x). Azimuthal bars (in **a**) span 50 px (104 μm) and were sampled over 25 x 25 px^2 (52 x 52 μm^2). The upper right portion of this crystal is 410 μm thick.

boundaries. This provides a means to distinguish between the two. Although rotational twinning conforms to specific boundaries that are dictated by the twinning relationship in distorted, ferroelastic UICs (this is discussed in Section 4.2.4), the absence of strain in the present system allows for additional twin boundaries. Nevertheless, both twinning and sectoring may be observable in a given crystal, and it is important to distinguish their effects on the optical properties of a given crystal.

When viewed along the urea channel, the orientation of the slow axis (the direction along which the refractive index is greatest) depends on crystal birefringence and optical rotation. The Metripol microscope provides a quantitative map of retardation, expressed as $|\sin \delta|$, in Figure 2.5b. As mentioned above, the five visible sectors (numbered in Figure 2.5) exhibit an alternating pattern in $|\sin \delta|$, as indicated by the pattern of blue and yellow-red sectors in the retardation image. With type A and B sectors defined as in Figure 2.3, this pattern corresponds to either A-B-A-B-A or B-A-B-A-B; although the identity of sectors in this crystal remains unknown, the pattern of retardation is consistent with the trigonal growth model in which the unit cell orientation remains constant over these five sectors. According to this model (Figure 2.3), if the "type A" faces expose type I, IV and III kink sites, then the "type B" faces should expose type II, IV and IV kink sites, and the molecular recognition should be different. (Of course, the opposite case is just as likely.) If rotational twins were present, the molecular recognition sites located at each growth face would be changed, and the alternating pattern would be interrupted. For this crystal, the "bimodal" pattern of retardation between sectors suggests the A-B-A (or B-A-B) pattern for a single unit cell orientation and a single sense of growth around the periphery of the crystal.

Nevertheless, it is important to point out subtle variations in |sin δ| exhibited by this crystal. In each of the three largest sectors, the retardation appears to change gradually as one moves closer to the growth face. In addition, these changes coincide with variations in the slow axis orientation, which are provided (by the azimuthal bars) in Figure 2.5a. Starting from sector 1 (at left), the angle between the slow axis and the growth face at the outer edges of the crystal is (approximately) 30°, 0°, 90°, 30°, and 60°. (From photomicrographs in Figure 2.4, it is clear in the orientation image that sector 1 has grown through a growth face that is oriented horizontally.) For the largest three sectors (#2-4), large variations in retardation are observable. In sector 2 (blue in Figure 2.5a), a horizontal ridge (most visible in Figure 2.4a-c) indicates a change in crystal thickness, but the height of the ridge in unknown. This ridge is clearly observable in Figure 2.4 and requires no further discussion. However, the topmost and top right sectors (#3 and 4) exhibit more gradual changes. In sector 3 (blue and turquoise in Figure 2.5a), the retardation changes, as does orientation, as one moves from crystal nucleus (at bottom) toward the edge. Unfortunately, the very small birefringence observed for this sector makes further analysis difficult; however, the upper right sector (colored yellow and green in Figure 2.5a), which exhibits greater values of |sin δ|, is amenable to such analysis.

For this sector (sector 4), variations in orientation are observable between crossed polars in Figure 2.4b and c. Qualitatively, the orientation of this sector changes appreciably as one moves from crystal nucleus to growth face. Chiral twinning is ruled out on the basis that the entire growth sector appears darkest at an analyzer rotation of +10° (Figure 2.4f). In the yellow region (near the nucleus) of the orientation image

(Figure 2.5a), the slow axis orientation is nearly parallel to the growth face. This is the same behavior observed in sector 2, which explains the similar retardations for these sectors. Toward the crystal face (the green region), this orientation changes substantially, and may be accompanied by a slight reduction in |sin δ|. Although |sin δ| for this sector is not homogeneous, the occurrence of regions of high retardation (red and orange) in Figure 2.5b appears reduced near the growth face so that these changes seem to coincide with changes in orientation. Unfortunately, their differences are quite small, and the relationship does not appear simple;[40] nevertheless, it is clear that on average, |sin δ| is increased somewhat near the nucleus, where the slow axis is oriented approximately parallel to the growth face.

Since UICs containing either pure 2,9-decanedione or 2-decanone are uniaxial, the optical anisotropy of this crystal appears to arise from a reduction in symmetry caused by the incorporation of *both* guests. Qualitatively, variations in birefringence observed between regions may be due either to differences in incorporated stoichiometry of 2,9-decanedione and 2-decanone or to differences in ordering of the two guests. It is possible that that guest populations change as a function of location within a given growth sector[14] (option 1); however, the observation of birefringence in this optically anomalous crystal suggests that the change in retardation could arise from variations in the occupancies of the different guest recognition sites irrespective of the overall composition of major and minor guests (option 2), or a combination of both. In a related study, Andrea Angott demonstrated[41] that UIC crystals containing mixtures of 2,9-decanedione and 2-decanone exhibit uniaxial crystal optics at elevated temperatures; under these conditions, guest disorder is presumed to occur, possibly in the form of rotational motions. Furthermore,

upon cooling to room temperature, birefringence was only partially recovered (if at all). These experiments suggest that anisotropic ordering of guests (option 2) is sufficient for optically anomalous behavior and that this order is not always recovered following heating. For the present crystal, sectors exhibiting large |sin δ| may simply incorporate guests in a more ordered fashion. However, the above evidence does not rule out contributions to decreased optical symmetry arising from differences in molecular incorporation (option 1).

The observation of curved sector boundaries provides an important clue to the nature of growth for this crystal. A crystal sector that grows faster than its neighbors will assume progressively smaller growth faces so that, given enough time, the sector boundaries grow together and the face disappears. For a sector that grows at a consistent rate, the sector boundaries will be straight; changes in the relative growth rate lead to curved boundaries or those that change direction. In photomicrographs of this crystal, sector boundaries for the upper right sector (and others) are quite curved, indicating changes in the rate of growth. Additionally, the curvature may be correlated with the modest changes in retardation discussed above. During faster growth it is conceivable that guest incorporation becomes more random because the selectivity between guests (and/or their ordering) that arises from differences in molecular recognition at the kink site is reduced. More random incorporation (or ordering) in this optically anomalous crystal should be observable as a decrease in retardation, while local variations in selectivity might contribute to a greater dispersion in the measured values. Of course, the presence of a variety of colors in the phase retardation map illustrates that this change is not homogeneous, but the occurrence of fewer regions of large |sin δ| as one moves

toward the growth face is consistent with a change in guest specificity at faster growth rates. However, a change in guest composition of the crystal growth solution may change both the rate of growth and retardation, so this bears further attention.

To this point, the optical properties of the three largest sectors have been rationalized according to the trigonal growth model. For these, an alternating pattern in retardation is observed between sectors whose boundaries coincide with the growth faces of the crystal. This observation favors growth sectoring over rotational twinning. In addition, there may be weak correlations between slow axis orientation (with respect to the growth face) and retardation as one moves from the center of the crystal toward the growth faces. Although rotational twinning does not appear to be present, variations in retardation within such regions (and between different sectors) may occur from differences in guest incorporation and/or ordering. Since it adjoins a type A sector, sector 5 (purple in Figure 2.17a) should incorporate guests similarly to sector 3; this assignment is in agreement with its low retardation. The average values of $|\sin \delta|$ (on the order of 0.2 to 0.3) observed sector 5 are somewhat greater than those observed in sector 3 (approximately 0.1 to 0.2), but both sectors exhibit smaller $|\sin \delta|$ values than those observed in sectors 2 and 4 (approximately 0.4 to 0.6). Although the trigonal growth model does not discuss *why* the optical properties can vary between similar sectors, it is reasonable that the orientation of the slow axis with respect to the growth face is linked to those optical properties. For sectors 3 and 5, subtle variations in guest occupancy and/or ordering may accompany the changes in slow axis orientation with respect to the growth face.

For sector 1 (colored red in Figure 2.5a), growth occurred through a horizontal face (see Figure 2.4a). In the absence of rotational twinning, this sector should have the same molecular recognition sites as sector 3 (also horizontal); it is therefore identified as the same sector type (A or B). In the retardation image (Figure 2.5b), the range of |sin δ| (~0.2 to 0.45) is comparable to |sin δ| within sectors 3 and 5, discussed above. (Again, differences in guest occupancy and/or ordering may give rise to higher values |sin δ| for this sector, the slow axis of which is oriented approximately 30° from the growth face.) This sector adjoins a small sector (observable in photomicrographs, Figure 2.4a and b) that possesses the same blue interference color as sector 2, which grew through a similarly oriented face. For this sector, the angle between the slow axis and the growth face is approximately 0°; although its birefringence has not been measured, this sector is predicted to incorporate and/or order guests in the same manner as sectors 2 and 4.

One final feature of the optical behavior exhibited by this crystal is worthy of discussion. In Figure 2.4g, a dark band is observed in the top left sector (assigned according to the crystal orientation in a; see arrow in g). This band intersects the growth face at an angle of approximately 55°. Although not easily discerned in Figure 2.4i, this band appears to be a dextrorotatory chiral twin. (Since chiral twins should intersect growth faces at 60° in this metrically trigonal crystal,[38] its orientation is not currently understood.) According to the growth mechanism proposed in Figure 2.3, dextrorotatory channels on this face should exhibit the same characteristics of guest incorporation as levorotatory channels that grew through adjacent faces (for instance, sector 3). In the retardation image (Figure 2.5), this chiral twin appears clearly visible (see arrow in Figure 2.5b). Although the resolution is poor, the phase retardation exhibited by this twin

appears similar to that of sector 3, in agreement with the growth mechanism. It is important to note that a UIC containing mostly 2,9-decanedione and some decane exhibits a substantial decrease in |sin δ| near chiral twin boundaries.[42] Unfortunately, this image does not permit the observation |sin δ| for the twin in an area removed from the chiral twin boundary. Another peculiarity of this chiral twin is that it appears to end abruptly at the ridge where the crystal thickness increases. This behavior is not understood.

The crystal described in Figures 2.4 and 2.5 demonstrates many interesting features and provides important evidence for the trigonal growth model. If the assignment of alternating sector type (either A-B-A-B-A or B-A-B-A-B) are correct, then it appears that this crystal grew through a single growth spiral. Unfortunately, this crystal was too small for guest content analyses via HPLC. However, future studies may provide crystals whose guest content can be quantified in order to determine if there is a correlation with optical properties. (Initial experiments conducted by Andrea Angott[43] require further refinements before any conclusions can be made.) Such studies will help elucidate the source of reduced optical symmetry in crystals such as this one and will be invaluable in rationalizing optical behavior in other crystals.

2.2.4 Crystals of Digonal Symmetry

2.2.4.1 Digonal Growth and Guest Zoning

Perhaps the most well-studied urea inclusion compound is 2,10-undecanedione/urea. This UIC yields commensurate ($3c_h' = 2c_g'$) crystals of orthorhombic ($C222_1$) symmetry. (Refer to Section 1.1.2 and Figure 1.3.) In the crystal

structure, the guests are related by a 2_1 screw axis along [001]. Hydrogen bonding tethers guest to host, and the methylene chain is oriented towards {100} channel faces. Such an alignment of guests distorts (or "strains") the unit cell from hexagonal metric symmetry by approximately 3.7% at room temperature to give an orthorhombic unit cell. This distortion is coupled to the crystalline optical properties: the largest refractive index (perpendicular to the channel axis) lies parallel to the strain and, hence, the orientation of the guest carbonyls. As with many ferroelastics, the presence of strain leads to twinned crystals; here, crystals contain nominally 12 rotational twins, of which adjacent twins are related to one another by ~60°. Figure 2.6a, taken from the work of Brown and Hollingsworth[44], presents a photomicrograph of a nearly perfect crystal in which each of the twelve rotational twins exhibits an interference color that corresponds to its slow axis orientation: yellow twins are oriented near the diagonal connecting NW and SE; blue twins are oriented near the diagonal between NE and SW; extinguished, magenta, twins are oriented horizontally. Figure 2.6b depicts the slow axis orientations for the sectors.

From this figure it is clear that the slow axis (and therefore the guest carbonyls) of each rotational twin is oriented approximately 60° to the growth face for a large portion of this crystal. For these regions, the angle of intercept at the growth face is always ~60°, so it was initially thought that such faces should expose identical functionality at their kink sites. However, closer inspection reveals this assumption is only approximate. The proposed mechanism (known as the digonal growth model) is schematized in Figure 2.6c-d, which includes kink sites 1-3 (which are located on faces 1-3 in Figure 2.6b) and assumes growth along a clockwise growth spiral. This figure was drawn in the same manner as Figure 2.3, and this discussion will use the same

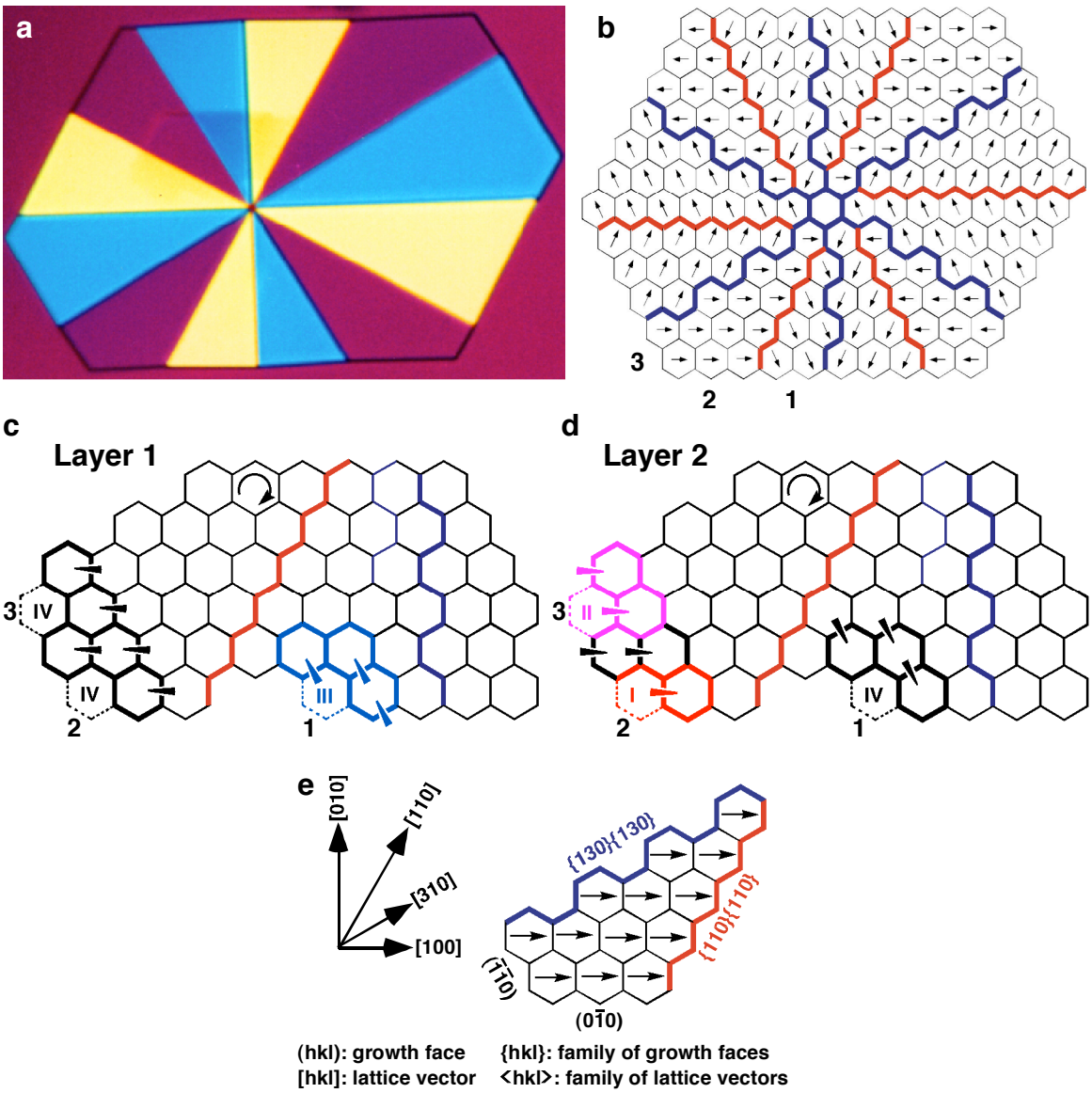

Figure 2.6 Rotational twinning in 2,10-undecanedione/urea. **(a)** Photomicrograph, taken between crossed polars and with λ plate, of a crystal exhibiting twelvefold sectoring. This view is along the [001] (channel) axis. The differently colored sectors are rotational twins; between adjacent twins the orientation of guest carbonyls' strain and the largest refractive index in the ab plane (which are all oriented parallel) differ by approximately 60°. **(b)** A schematic of the rotational twinning present in the crystal. Slow axis orientations are indicated by the arrows, which also denote [100] for each sector. Note that the rotational twin boundaries are in many cases not congruent with the growth faces. **(c–d)** Proposed growth mechanism. These cartoons of kink sites 1–3 represent two guest layers present in each commensurate repeat. (Similar diagrams were provided for 2,9-decanedione/urea in Figure 2.3.) The wedges indicate urea N–H for each underlayer, which form hydrogen bonds with guests there. Because kink sites 1, 2 and 3 (dotted lines) expose different molecular functionality at the crystal surface, differential zoning and/or ordering of guests may occur between rotational twins (e.g., 1 vs. 2) and between portions of the same twin that form through different growth faces (e.g., 2 vs. 3 – see text). **(e)** Index of the sector at lower left (in **a** and **b**). Here, relevant lattice vectors and growth faces are provided. Boundaries between sectors are labeled according to the convention used here (see Figure 4.2). The image in **a** is taken from Brown and Hollingsworth, *Nature (London)*, **376**, 323-327, (1995); schematic **b** was drawn by Mark D. Hollingsworth.

terminology introduced in Section 2.2.3.1. Like 2,9-decanedione (Figure 2.3), guest carbonyls form hydrogen bonds with ureas along appropriate channel walls of the underlayer; these are denoted in Figure 2.6 by the solid wedges. For 2,10-undecanedione/urea there are two guests per commensurate repeat, so two layers must be considered. In the first layer (Figure 2.6c), the donor urea exposed at kink site 1 is oriented 120° from the direction of growth (type III), while kink sites 2 and 3 both exhibit no donor ureas (type IV). In the second layer (Figure 2.6d), kink site I is type IV, kink site 2 is type I (donor urea oriented with direction of growth) and kink site 3 is type II (donor urea oriented 60° from direction of growth).

Summing these up, kink sites 1, 2 and 3 should exhibit different patterns of guest incorporation and/or ordering because none of them possesses identical donor ureas over the course of each commensurate repeat. Over the entire crystal, sectors whose slow axis intersects the growth face at 60° alternate between types 1 and 3, while sectors for which the slow axis is parallel to the growth face are always type 2. The work discussed below demonstrates that although sectors grown through type 1 and 3 faces do not exhibit substantial differences in guest incorporation, significant differences in guest content can be found between these and sectors grown via type 2 faces.

2.2.4.2 HPLC Evidence of Guest Zoning

For UICs containing mixtures of 2,10-undecanedione and 2-undecanone, high performance liquid chromatography has been instrumental in studying guest zoning. The HPLC owned by Professor Christopher T. Culbertson of the KSU Department of Chemistry was used for these experiments; it consists of a Waters 2690 autosampler and

pump coupled to a Waters 486 UV detector and DuPont Zorbax ODS C_{18} column (4.6 mm by 25 cm in length; 5 μm beads). Millenium-32 *v*. 3.05.01 (for Windows) software was used for device control and data analysis. A fixed eluent of 24% water, 40% acetonitrile, and 36% methanol was used with a flow rate of 1 mL min^{-1}. (The organic solvents were HPLC "gradient grade," and the water was deionized using a Barnsted filtration system.) Using this system, 2,10-undecanedione and 2-undecanone elute at approximately 3.7 and 10.2 minutes, respectively. (Sample chromatograms and a calibration curve are provided in Figure 7.11.) For these guests, the UV detector was set at 275 nm. (Andrea Angott demonstrated[45] λ_{max} = 275 nm for 2,9-decanedione in a similar solvent mixture.) Using this system, crystal fragments with approximate masses of 0.1 mg could be analyzed reliably; typically, up to four 50 μL injections of each sample were performed. Periodically, a standard (containing a known ratio of mono- and diketone guest) was injected to monitor HPLC performance and to help establish the limits of accuracy for the sample injections.[46] For the experiments described below, six 25 μL injections of a methanol solution containing approximately 75:25 2,10-undecanedione:2-undecanone (the concentration of which is on the order of the guest concentrations for the dissolved crystal sectors) were injected at various times during analysis of the crystals.[47] Integration of the chromatogram peaks gave 73.7 (0.2)% diketone fraction. For the sample injection data, the precision in measurements is presumed to be equivalent to or better than 0.5% (guest content).

Figure 2.7 provides the results of two such experiments. To probe for guest zoning, these crystals were cleaved so that portions of twins extending over more than one growth sector were separated. As discussed in Figure 2.6, for UICs based on 2,10-

undecanedione, there are three types of growth faces for which intersectoral zoning is possible. Sectors that grow through a type 1 or 3 face have their largest refractive index and guest carbonyls oriented approximately 60° to the growth face. These sectors differ according to how that axis is oriented with respect to the growth spiral, which is assumed constant for the entire crystal. (Here, assignments were made according to the convention established in Figure 2.6 and assume a CW growth spiral; for a potential CCW growth spiral, the assignments provided in parentheses apply.) As illustrated in Figure 2.6, for many crystals, a majority of the crystal volume is occupied by this {110} type of face. For sectors grown along a type 2 face, the slow axis (and, therefore, guest carbonyls) is oriented parallel (or nearly so) to the growth face. The crystal in Figure 2.7a had six rotational twins that were cleaved from each other and along the growth sector boundaries to produce a total of nine sectors. Of these, eight were type 1 or 3 (four each), and one was type 2. HPLC analysis of the four type 1(3) sectors provides a mean 2,10-undecanedione fraction of 83.6 (0.3)% with a range of 83.3% – 83.9%. For four type 3(1) sectors, the average diketone content was 83.5 (0.6)% with a range of 82.8 – 84.3%. For type 1 and 3 sectors, the guest content therefore does not appear to differ significantly. (Combining all eight type 1(3) sectors, the mean diketone content was 83.6 (0.4)%.) The small size of these individual sectors limited each sample to a single injection (in 50 μL methanol), so no data on the precision of these measurements is available. This also makes a comparison of trends between sectors and faces difficult; nevertheless, guest content within these sectors appear to differ somewhat from that of the type 2 fragment (c), for which 84.9% diketone was measured.

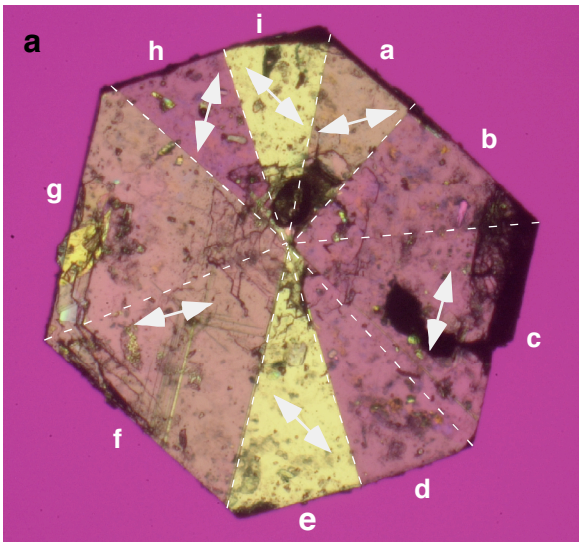

Sector	Type	Diketone (%)
a	1 (3)	83.9
b	3 (1)	83.6
c	2	84.9
d	1 (3)	83.5
e	3 (1)	82.8
f	1 (3)	83.6
g	3 (1)	84.3
h	1 (3)	83.3
i	3 (1)	83.4

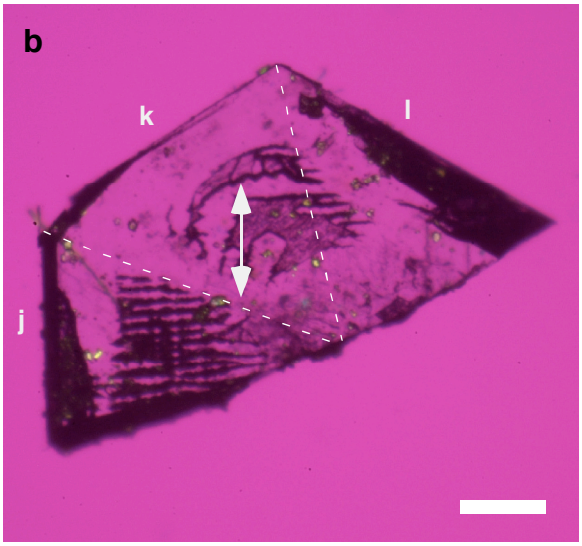

Sector	Type	Diketone (%)
j	2	80.3
k	1 (3)	78.2
l	3 (1)	78.6

Figure 2.7 Intersectoral zoning in UICs containing 2,10-undecanedione and 2-undecanone. Photomicrographs taken between crossed polars and with λ plate of a pair of crystals grown from a 75:25 (**a**) and an 80:20 (**b**) mixture of 2,10-undecanedione and 2-undecanone in methanol. Scale bar = 0.50 mm (Nikon 1.3x). Double-headed arrows represent the slow axis orientations (and therefore <100>) in each sector. The tables provide assignments of kink site type (based on a CW growth spiral) according to the convention of Figure 2.6. (Assignments in parentheses assume a CCW growth spiral.) Cleavage of the crystals was performed with an X-acto blade according (approximately) to the dotted lines. (For crystal **b**, the location of the nucleus was assumed.) HPLC of the individual sectors (one injection each) following cleavage provides the amounts of 2,10-undecanedione in the tables. Errors in each analysis are estimated at less than 0.5% from four runs of a sample of known guest concentration. (See text.) For crystal **a**, four type 1 (3) sectors gave 83.6 (0.3)% diketone; for four type 3 (1) sectors, the mean diketone content was 83.5 (0.6)%. Combined, these eight sectors contain 83.6 (0.4)% diketone, while type 2 sector c revealed 84.9% diketone. For crystal **b** the guest content within type 1 (3) and 3 (1) sectors (k and l) was not significantly different. Here, type 2 sector j incorporated 1.9% more diketone than the mean, 78.4 (0.3)%, of sectors k and l.

Figure 2.7b provides a second crystal for which a similar analysis was performed. Dissection according to the presumed location of the crystal nucleus (approximate cleavage locations are depicted in the figure with dotted lines) produced three sectors: one type 2 (j) and two type 1(3) (k and l) sectors. HPLC analysis of these, performed as above, provides the guest fractions presented in the table. Here, the pair of type 1(3) faces exhibit very similar diketone contents (78.2 and 78.6%, respectively). Combined, sectors k and l average 78.4 (0.3)% of 2,10-undecanedione. Although based on only two injections, this mean value is appreciably different from 80.3% diketone fraction measured in sector j. As with the first crystal, this small difference in guest content (~1.9%) appears significant so that guest zoning can be identified between growth faces where the slow axis is oriented ~60° (types 1 and 3) and ~0° (type 2) from the growth face. Like the crystal described in Figure 2.7a, this crystal appears to incorporate guests according to the digonal growth model.

In both crystals, type 1 and 3 sectors exhibit very similar guest concentrations. Furthermore, in crystals a and b, the average fraction of diketone in type 1 and 3 sectors was less than the diketone fraction observed for the type 2 sector by 1.3 and 1.9%, respectively. Although these results are suggestive, further work in which the statistical significance of both sets of concentrations (i.e. from sector types 1(3) and 2) are required before firm conclusions can be made. In work[10,11,48] that ultimately led to the current understanding of preferential incorporation and the growth of solid solutions, Lahav, *et al*. demonstrated comparatively small (yet significant) differences in impurity incorporation. Thus, population differences on the order of 1-2% can be considered affirmative evidence of guest zoning.

2.3 Discussion

This chapter describes several important observations on crystal growth processes and their effect on macroscopic UIC crystal habit. One interesting feature of urea inclusion compounds is that they exhibit differential incorporation and/or ordering between structurally similar guests. These phenomena are a consequence of the reduced symmetry at the crystal growth face and the differences in molecular recognition sites exposed at growth faces that differ in symmetry. UICs containing mixtures of 2,9-decanedione and 2-decanone are optically anomalous: they retain trigonal metric symmetry while demonstrating lower (biaxial) optical symmetry. Such behavior has been measured via optical methods.

Crystals containing mostly 2,10-undecanedione and a guest impurity present a different picture of guest inclusion: because their unit cells are distorted from high symmetry by the orientation of the guest carbonyls towards the urea channel walls, a decrease in the number of diketones results in a reduction in strain (which could be described as a shift toward higher *metric* symmetry). However, because the incorporation of guest impurities appears to occur in a non-random fashion (as suggested by HPLC analysis), the impurity actually reduces the nominally orthorhombic ($C222_1$) symmetry. Thus, the preferential incorporation of this guest at particular kink site morphologies leads to distinctive guest ordering and symmetry reduction.

As the remaining chapters will demonstrate, an understanding of guest ordering is important for investigating the ferroelastic properties of solid materials such as urea inclusion compounds. Disparities in guest ordering or composition across twin or sector boundaries can influence the properties one is trying to study; alternatively, they can be

exploited to tailor those properties. Ultimately, the process by which a material is constructed (for this discussion, crystal growth) can dictate its physical properties. The prudent "crystal engineer" should be aware of this process as it provides an important handle by which the macroscopic properties of crystalline materials may be studied and manipulated.

References Cited

1. Kahr, B. & McBride, J. M. Optically anomalous crystals. *Angew. Chem. Int. Ed.* **31**, 1-26 (1992).
2. Hulliger, J. Chemistry and crystal crowth. *Angew. Chem. Int. Ed.* **44**, 143-162 (1994).
3. Frenkel, J. On the surface motion of particles in crystals and the nature roughness of crystalline faces. *J. Phys. U.S.S.R.* **9**, 392-398 (1945).
4. Burton, W. K., Cabrera, N. & Frank, F. C. The growth of crystals and the equilibrium structures of their surfaces. *Philos. Trans. Roy. Soc. Lond.* **243**, 299-358 (1951).
5. Buckley, H. E. *Crystal Growth*, (John Wiley & Sons, Inc., New York, 1951), pp. 339-387.
6. Wust, T., Gervais, C. & Hulliger, J. How symmetrical molecules can induce polarity: On the paradox of dilution. *Cryst. Growth Des.* **5**, 93–97 (2005).
7. McBride, J. M. Symmetry reduction in solid solutions: A new method for materials design. *Adv. Mater.* **1**, 87-89 (1989).
8. Vaida, M., Shimon, L. J. W., Van Mil, J., Ernst-Cabrera, K., Addadi, L., Leiserowitz, L. & Lahav, M. Absolute asymmetric photochemistry using centrosymmetric single crystals. The host/guest system (E)-cinnamamide/E-cinnamic acid. *J. Am. Chem. Soc.* **111**, 1029-1034 (1989).
9. Vaida, M., Shimon, L. J. W., Weisinger-Lewin, Y., Frolow, F., Lahav, M., Leiserowitz, L. & McMullan, R. K. The structure and symmetry of crystalline solid solutions: A general revision. *Science (Washington, D. C.)* **241**, 1475-1479 (1988).
10. Weissbuch, I., Addadi, L., Lahav, M. & Leiserowitz, L. Molecular recognition at crystal interfaces. *Science (Washington, D. C.)* **253**, 637-645 (1991).
11. Weissbuch, I., Addadi, L., Berkovitch-Yellin, Z., Gati, E., Weinstein, S., Lahav, M. & Leiserowitz, L. Centrosymmetric crystals for the direct assignment of the absolute configuration of chiral molecules. Application to the α-amino acids by their effect on glycine crystals. *J. Am. Chem. Soc.* **105**, 6615-6621 (1983).
12. Addadi, L., Berkovitch-Yellin, Z., Weissbuch, I., Lahav, M. & Leiserowitz, L. A link between macroscopic phenomena and molecular chirality: crystals as probes for the direct assignment of absolute configuration of chiral molecules. *Top. Stereochem.* **16**, 1-85 (1986).
13. McBride, J. M. & Bertman, S. B. Using crystal birefringence to study molecular recognition. *Angew. Chem. Int. Ed.* **28**, 330-333 (1989).
14. Kahr, B. & Gurney, R. W. Dyeing Crystals. *Chem. Rev.* **101**, 893-951 (2001).
15. Touryan, L. A., Clark, R. H., Gurney, R. W., Stayton, P. S., Kahr, B. & Vogel, V. Incorporation of fluorescent molecules and proteins into calcium oxalate monohydrate single crystals. *J. Cryst. Growth* **233**, 380-388 (2001).
16. Vetter, W. M., Totsuka, H., Dudley, M. & Kahr, B. The perfection and defect structure of organic hourglass inclusion K_2SO_4 crystals. *J. Cryst. Growth* **241**, 498-506 (2002).

17. Sours, R. E., Fink, D. A. & Swift, J. A. Dyeing uric acid crystals with methylene blue. *J. Am. Chem. Soc.* **124**, 8630-8636 (2002).
18. Gurney, R. W., Mitchell, C. A., Ham, S., Bastin, L. D. & Kahr, B. Salting Benzenes. *J. Phys. Chem. B* **104**, 878-892 (2000).
19. Kahr, B., Kaminsky, W. & Claborn, K. Why biphenyl configuration still matters. *J. Phys. Org. Chem.* **17**, 735-739 (2004).
20. Welberry, T. R. & Mayo, S. C. Diffuse X-ray scattering and Monte-Carlo study of guest-host interactions in urea inclusion compounds. *J. Appl. Crystallogr.* **29**, 353-364 (1996).
21. Harris, K. D. M., Smart, S. P. & Hollingsworth, M. D. Structural properties of α,ω-dibromoalkane/urea inclusion compounds: a new type of interchannel guest molecule ordering. *J. Chem. Soc., Faraday Trans.* **87**, 3423-3429 (1991).
22. Lauritzen, J. I., Jr. Analysis of dielectric loss in two urea addition compounds: the hindered single-axis polar rotator. *J. Chem. Phys.* **28**, 118-131 (1958).
23. Aakeröy, C. B. & Seddon, K. R. The hydrogen bond and crystal engineering. *Chem. Soc. Rev.* **22**, 397-407 (1993).
24. Hollingsworth, M. D. Personal communication to J. R. Rush (2002).
25. Hollingsworth, M. D., Brown, M. E., Hillier, A. C., Santarsiero, B. D. & Chaney, J. D. Superstructure control in the crystal growth and ordering of urea inclusion compounds. *Science (Washington, D. C.)* **273**, 1355-1359 (1996).
26. Hollingsworth, M. D. Personal communication to J. R. Rush (2006).
27. Schlenk, W., Jr. Asymmetric urea inclusion lattice. IV. Absolute configuration of the lattice. *Liebigs Ann. Chem.* **7**, 1195-1209, (1973). This work was discussed by Hollingsworth, M. D. & Harris, K. D. M. "Urea, thiourea, and selenourea" in *Comprehensive Supramolecular Chemistry*, vol. 6 (eds. MacNicol, D. D., Toda, F. & Bishop, R.) (Pergamon Press, New York, 1996) pp. 177-237.
28. Kaminsky, W., Claborn, K. & Kahr, B. Polarimetric imaging of crystals. *Chem. Soc. Rev.* **14**, 1-12 (2004).
29. McCrone, W. C. "Polymorphism" in *Physics and Chemistry of the Organic Solid-State*, (eds. Fox, D., Labes, M. M. & Weisemberg, A.) (Interscience, New York, 1965) p. 725.
30. Glazer, A. M., Lewis, J. G. & Kaminsky, W. An automatic optical imaging system for birefringent media. *Proc. R. Soc. Lon. Ser. A* **452**, 2751-2765 (1996).
31. Johannsen, A. *Manual of Petrographic Methods*, (McGraw-Hill Book Company, New York, 1918), pp. 343-346.
32. Geday, M. A., Kaminsky, W., Lewis, J. G. & Glazer, A. M. Images of absolute retardance $L \bullet \Delta n$, using the rotating polariser method. *J. Microsc.* **198**, 1-9 (2000).
33. Oxford Cryosystems, Ltd. The Metripol birefringence imaging system. *Accessed November 31, 2005 at* http://www.metripol.com.
34. Wood, E. A. *Crystals and Light*, (Dover Publications, Inc., New York, 1977), pp. 112-123.
35. Gay, P. *An Introduction to Crystal Optics*, (Longmans, London, 1967), pp. 115-119.
36. Abel, M. J. Laboratory notebook entry mja-a-31-4. (2002).

37. Schlenk, W., Jr. Rotation of the plane of polarized light by hexagonal urea inclusion crystals. *Chem. Ber.* **101**, 2445-9 (1968).
38. Hollingsworth, M. D., Brown, M. E., Dudley, M., Chung, H., Peterson, M. L. & Hillier, A. C. Template effects, asymmetry, and twinning in helical inclusion compounds. *Angew. Chem. Int. Ed.* **41**, 965-969 (2002).
39. Peterson, M. L. Laboratory notebook entry mlp-c-287-4. (2001).
40. Rush, J. R. Laboratory notebook entry jrr-f283. (2007).
41. Angott, A. M. Exploration of phase transitions and sector differences in urea inclusion compounds. *Kansas State University/NSF-REU report* (2003).
42. Rush, J. R. & Hollingsworth, M. D. Unpublished observations. This crystal was studied on laboratory notebook page jrr-b088. (2003).
43. Angott, A. M., Rush, J. R. & Hollingsworth, M. D. Unpublished observations. This crystal was studied on laboratory notebook page ama-a055. (2003).
44. Brown, M. E. & Hollingsworth, M. D. Stress-induced domain reorientation in urea inclusion compounds. *Nature (London)* **376**, 323-7 (1995).
45. Angott, A. M. Laboratory notebook entry AMA-A-29. Also discussed on jrr-b099-2. (2003).
46. Rush, J. R. Laboratory notebook entry jrr-f228. (2006).
47. Rush, J. R. Laboratory notebook entries jrr-c130-1, jrr-c130-3, jrr-c133-1, jrr-c133-5, jrr-c133-10, jrr-c133-14. (2004).
48. Addadi, L., Berkovitch-Yellin, Z., Weissbuch, I., Van Mil, J., Shimon, L. J. W., Lahav, M. & Leiserowitz, L. Growth and dissolution of organic crystals with tailor-made inhibitors - Implications in stereochemistry and materials science. *Angew. Chem. Int. Ed.* **24**, 466-485 (1985).